Available online at www.sciencedirect.com
ScienceDirect
Trans. Nonferrous Met. Soc. China 24(2014) 243−249
Transactions of Nonferrous Metals Society of China
www.tnmsc.cn

Variation of soda content in fine alumina trihydrate by seeded precipitation

Gui-hua LIU, Peng WANG, Tian-gui QI, Xiao-bin LI, Lü TIAN, Qiu-sheng ZHOU, Zhi-hong PENG

School of Metallurgy and Environment, Central South University, Changsha 410083, China

Received 2 December 2012; accepted 26 April 2013

Abstract: High soda content in fine alumina trihydrate(ATH) limits its application and increases the soda consumption. The variation of soda content in the fine ATH by seeded precipitation was determined by detection of electric conductivity of solution, soda content in ATH, measurement of particle size distribution and microscopic analysis. The results show that high concentration of sodium aluminate solution, ground circulative seed, low temperature or fast initial precipitation rate increases the soda content in ATH. Soda mainly exists in lattice soda and less soda in desilication product (DSP) exists in the fine ATH precipitated from sodium aluminate solution with concentration of Al_2O_3 ($\rho_{Al_2O_3}$) more than 160 g/L and mass ratio of alumina to silica (μ_{SiO_2}) of 400, and lattice soda decreases with increasing initial precipitation temperature, aging seed, and low precipitation rate and precipitation time. Results also imply that $Na^+Al(OH)_4^-$ ion-pair influences lattice soda content in ATH on the basis of electric conductivity variation.

Key words: alumina trihydrate; seeded precipitation; soda content; lattice soda; sodium aluminate solution

1 Introduction

Fine alumina trihydrate (ATH) is not only used as the raw material of alumina-based ceramic and catalyst carrier, but also as the main filler of environmental friendly flame retardant, artificial agate and so on. Compared with neutralization and alkoxide hydrolysis for preparing fine ATH, the seeded precipitation from sodium aluminate solution has a lot of advantages, such as low cost, spent-liquor circulation and less pollution. But high soda (expressed in Na_2O) content in ATH from sodium aluminate solution limits its application. High concentration solution ($\rho(Na_2O)$>160 g/L), rather than low concentration solution, is often employed in seeded precipitation for digestion of diasporic bauxite in China [1], leading to high soda content (Na_2O 0.3%−0.7%) in ATH. So the variation of the soda content in ATH is essential for reducing the soda content of the fine ATH, and for understanding the mechanism of seeded precipitation in production of smelter grade alumina.

Soda in ATH exists in three forms: lattice soda (inserted in lattice), soda in DSP and adsorption soda (adsorbing on the surface of ATH), but only the third can be washed with boiling water. Diluting solution, elevating temperature, controlling seed coefficient φ (the mass ratio of alumina in seed to alumina in solution) or varying particle size of seeds can slightly reduce the soda content of the coarse ATH [2,3]. However, soda content in ATH is not clear so far for the co-existence of many kinds of soda in ATH from industrial aluminate solution. Many researches focus on the influence of cation on mechanism of particle growth and on particle agglomeration in preparation of coarse ATH. FLEMING et al [4] studied the structure of gibbsite and the occurrence of Na^+ and K^+ in crystals by computer modeling techniques, and suggested that cation incorporation benefited the elongation of the prismatic faces. FREIJ and PARKINSON [5] reported that Na^+ was located in (001) face between two layers of crystal during the crystallization process. LOH et al [6] and PRESTIDGE and AMEOV [7] reported that Na^+ benefited agglomeration while K^+ and Cs^+ improved nucleation. BLAGOJEVIĆ et al [8] found that Na^+ was adsorbed on the surface of the ATH and then inserted into particle during agglomeration process in the low concentration, and that soda content in ATH of particle size <45 μm is more than that of particle size of 45−63 μm, and that soda content reduced with addition of seeds due to the inhibition of agglomeration. GAN and

Foundation item: Project (51274242) supported by the National Natural Science Foundation of China
Corresponding author: Tian-gui QI; Tel: +86-731-88877830; E-mail: qitiangui@csu.edu.cn
DOI: 10.1016/S1003-6326(14)63053-3

FRANKS [9] found that the most active protons and oxygen atoms in crystal were located in (001) face, implying that the distribution of atoms on surface may affect the soda content in ATH. The above experiments were generally carried out under low concentration ($\rho(Na_2O)$<150 g/L) with either large seed coefficient or no seed. Researchers focused on the cation's behavior in growth and agglomeration rather than the variation of soda content in ATH.

This work mainly studied the variation of precipitation ratio, precipitation rate, particle size distribution (PSD) and soda content in the fine ATH from the high concentration solution, and discussed the dependence of lattice soda content on the precipitation ratio, precipitation rate, PSD, morphology of ATH and solution structure.

2 Experimental

2.1 Preparation of raw material

Sodium aluminate solution for seeded precipitation was made from industrial grade alumina trihydrate ($Al(OH)_3$>98% in mass fraction, CHALCOA) and spent liquor (from an alumina refinery in Henan province, China), and μ_{Si} (mass ratio of alumina to silica in solution) of pregnant liquor was 400±30 after desilication in sodium aluminate solution by adding lime in analytically pure grade (AR grade). Sodium aluminate solution for electrical conductivity measurement was made from alumina trihydrate (AR grade) and sodium hydroxide (AR grade). Seed was made from the reaction of sodium aluminate solution (ρ_{Na_2Ok}=165.26 g/L, $\rho_{Al_2O_3}$= 177.08 g/L) with sulphuric acid (0.5 mol/L). Other reagents were in AR grade.

2.2 Analysis method

The concentrations of Na_2O and Al_2O_3 in solution were measured by titration, the concentration of SiO_2 was determined with SP−752 UV-V15 spectro-photometer (Spectrum Shanghai, Ltd), Na_2O content in ATH was detected by Flame Photometer (Shanghai AOPU Analytical Instr. Co., Ltd), electrical conductivity of solution was carried out with DDSJ−308A conductivity meter (Shanghai REX Instrument Factory) at 25 °C, PSD of ATH was finished on Mastersizer 2000 laser particle size analyzer (Malvern, British), and morphology of ATH was observed by JSM−6360V scanning electron microscope (JEOL , Japan).

2.3 Procedures

1000 mL pregnant liquor was transferred into a stainless steel tank with a volume of 1200 mL (Heating in water bath, temperature accuracy ±0.5 °C, stirring speed controlled by electric motor), and seed with φ=0.07−0.1 was then added. Sample was sucked from the tank by piette and then centrifuged. The concentrations of Na_2O_k, Al_2O_3 and SiO_2 in sodium aluminate solution were determined. The fine ATH was washed with boiling water until pH ~9 of washing water, and the washed ATH was then dried at 80 °C for PSD measurement and morphology observation.

3 Results and discussion

3.1 Influence of Al_2O_3 concentration of solution on soda content of ATH

Pregnant liquor with high concentration (ρ_{Na_2Ok}>160 g/L, $\rho_{Al_2O_3}$>170 g/L) is adopted in the treatment of diasporic bauxite in China, while their concentrations are low (ρ_{Na_2Ok}<145 g/L, $\rho_{Al_2O_3}$<155 g/L) in the treatment of gibbsite bauxite by Bayer process at abroad. Reaction behavior of aluminate anion in seeded precipitation process is influenced remarkably by the concentration of sodium aluminate solution. The effect of concentration of Al_2O_3 in solution on soda content of ATH is listed in Table 1.

Table 1 Effect of alumina concentration on PSD and soda content in ATH

Sample No.	Pregnant liquor concentration/ ($g\cdot L^{-1}$)		PSD/μm			$\eta_{Al_2O_3}$/ %	Na_2O content/ %
	Al_2O_3	Na_2O	$d(0.1)$	$d(0.5)$	$d(0.9)$		
1	133.28	124.50	0.437	0.672	1.384	58.45	0.215
2	148.00	140.25	0.193	0.256	0.496	59.09	0.205
3	156.18	147.75	0.249	0.351	0.632	57.35	0.271
4	177.08	165.26	0.191	0.248	0.430	53.21	0.332

φ=0.07, temperature 45 °C, time 48 h, stirring rate 500 r/min

As shown in Table1, a decreasing precipitation ratio $\eta_{Al_2O_3}$, $\eta_{Al_2O_3}=(\rho_{init}-\rho_{end})/\rho_{init}$, where ρ_{init} and ρ_{end} are Al_2O_3 concentrations in pregnant liquor and spent liquor, respectively, can be observed with increasing Al_2O_3 concentration under the same experiment condition. And the soda content in the fine ATH rises with increasing Al_2O_3 concentration. For example, the soda content of ATH is 0.332% at $\rho_{Al_2O_3}$=177.80 g/L, while only 0.205% at $\rho_{Al_2O_3}$=148.00 g/L. Although the above variation of soda content in ATH is consistent with that in producing fine low soda ATH from the low concentration solution [10,11], it costs much by diluted aluminate solution in China due to the expensive evaporation of excess water and the low productivity of ATH per unit volume.

3.2 Influence of circulative seed on PSD and purity of alumina trihydrate

Circulative seed can prevent other impurities from

transforming into the spent liquor and simplify process in the seeded precipitation. Since particle agglomeration is promoted intently in the production of coarse ATH when many seeds were added, the grinding circulative seed with φ about 0.1 were employed to avoid particles agglomeration in preparation of fine ATH. Influence of circulative seeds on soda content of production can be seen in Table 2.

Table 2 Effect of seed type on PSD and soda content of $Al(OH)_3$

Seed cycle	$\eta_{Al_2O_3}$/%	Specific surface area/($m^2 \cdot g^{-1}$)	PSD/μm			Impurity content/%	
			$d(0.1)$	$d(0.5)$	$d(0.9)$	Na_2O	SiO_2
1st	48.57	2.34	0.872	2.944	7.539	0.512	0.031
2nd	46.45	2.04	0.748	8.019	13.285	0.561	0.016
3rd	47.99	1.98	0.764	8.235	13.525	0.452	0.006

Pregnant liquor: $\rho_{Na_2O_k}$=159.78 g/L, $\rho_{Al_2O_3}$=174.17 g/L; φ≈0.1; Grinding time of seed about 1 h; precipitation temperature 45 °C; precipitation time 48 h

Table 2 indicates that the PSD of ATH increases but specific surface area decreases with addition of the grinding circulative seeds, and the particle sizes of the 1st, 2nd and 3rd all become coarse compared with particle sizes in Table 1. In addition, soda content of ATH increases sharply in comparison with the data in Table 1.

SEM images of ATH from the grinding circulative seeds and fresh seeds are given in Fig. 1

Results in Fig.1 show that ATH appears in irregular shape and particle sizes are not uniform with the addition of the grinding circulative seeds. In addition, particles agglomeration also can be seen, resulting in decreases of the specific surface area. In contrast, ATH presents in flake shape and particle sizes are uniform with the addition of fresh seeds, and no remarkable agglomeration of particles is observed. The above results in Table 2 and Fig. 1 suggest that the inhibition of agglomeration benefits to reducing soda content in ATH. Therefore variation of soda content can be explained as follows: 1) irregular surface promotes the adsorption of Na^+ ion on (001) face of crystal [9,12]; 2) agglomeration of particle also influences soda content packed in capillary of the coarse ATH.

3.3 Influence of precipitation temperature scheme on soda content of ATH

The precipitation ratio and quality of ATH were influenced by temperature. Low temperature leads to low solubility of ATH, high productivity, high precipitation rate and limitation of agglomeration. High precipitation temperature, however, often promotes agglomeration and growth of particle. Two series of temperature schemes, constant temperature and variable temperature, were

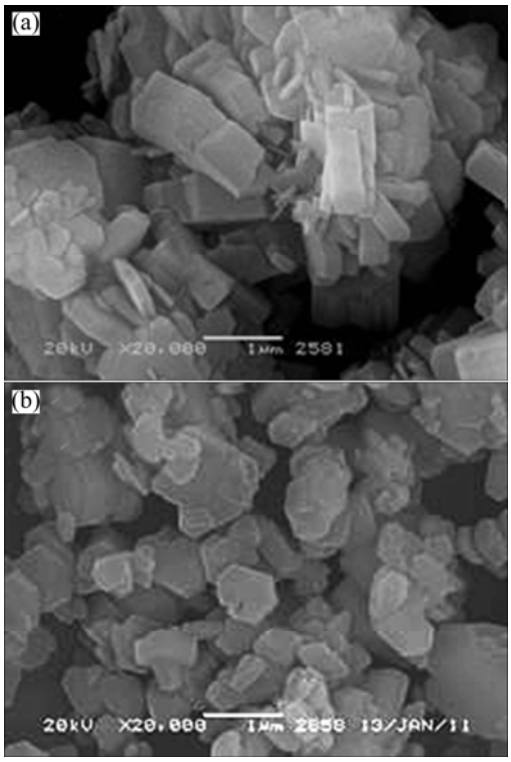

Fig. 1 SEM images of ATH from seeded precipitation with addition of seeds: (a) Grinding circulative seeds, grinding time 1 h, φ≈0.1, precipitation temperature 45 °C, precipitation time 48 h; (b) Fresh seeds, φ≈0.07, temperature 45 °C, time 48 h, stirring rate 500 r/min

carried out in seeded precipitation for preparation of fine ATH, and dependence of precipitation ratio on temperature scheme are plotted in Fig. 2.

Precipitation ratio at variable temperature scheme is less than that at constant temperature when the end temperature is the same in seeded precipitation (in Fig. 2). For example, precipitation ratio reaches 35% at

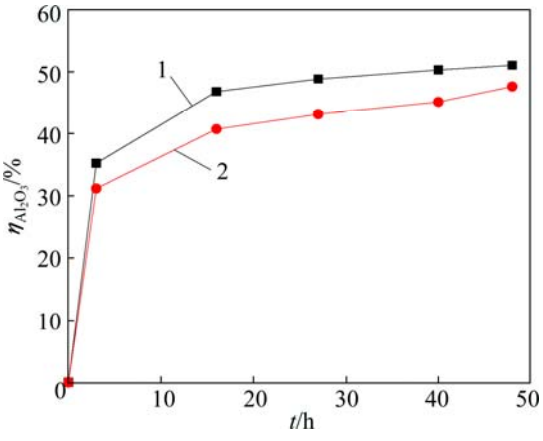

Fig. 2 Influence of temperature scheme on precipitation ratio in ATH (ρ_{Na_2Ok}=168.64 g/L, $\rho_{Al_2O_3}$=176.44 g/L, φ≈0.07): 1—45 °C for 48 h; 2—55 °C for 10 h, 50 °C for 16 h and 45 °C for 22 h

45 °C for 3 h, as shown in curve l of Fig. 2, while 31% at the initial temperature of 55 °C. And precipitation ratio reaches 51.03% at 45 °C for 48 h, as shown curve l of Fig. 2, while only 47.61% can be seen at variable temperature for 48 h, as shown in curve 2 of Fig. 2.

To relate precipitation rate to soda content of the fine ATH, data from precipitation ratio−time curves in Fig. 2 are fitted, and the fitting function is then differentiated to obtain the precipitation rate listed in Table 3.

Table 3 Relationship of precipitation rate and time in seeded precipitation

Sample No.	Formula of simulation equation	Precipitation rate, $d\eta/dt$				
		3 h	16 h	27 h	40 h	48 h
1	$\eta_{Al_2O_3}=5.73\ln(1+173.99t)$	1.90	0.36	0.21	0.14	0.12
2	$\eta_{Al_2O_3}=5.65\ln(1+82.51t)$	1.88	0.35	0.21	0.14	0.12

As shown in Table 3, precipitation rate goes down sharply at the beginning, and then decreases slowly after 27 h, meaning that more ATH is precipitated quickly at the beginning. In addition, the initial precipitation rate of sample 1 is slightly higher than that of sample 2.

The PSD and specific surface area of ATH at 3 h and 48 h are presented in Table 4.

Table 4 Results of PSD and specific surface area at initial and end of seeded precipitation

Sample No.	Time/h	PSD/μm			Specific surface area/($m^2 \cdot g^{-1}$)
		$d(0.1)$	$d(0.5)$	$d(0.9)$	
1	3	0.750	3.834	6.755	2.82
	48	0.833	3.934	6.756	2.635
2	3	0.747	3.864	6.858	2.82
	48	0.836	4.116	7.077	2.57

Particle size of fine ATH in Table 4 increases slightly but the specific surface area decreases when seeded precipitation undergoes from 3 h to 48 h. It implies that particle agglomeration is limited at low φ, large $\eta_{Al_2O_3}$ and suitable temperature. In addition, sample 2 under variable temperature scheme has a smaller specific surface compared with sample 1 at a constant temperature.

The adsorption soda on the surface of ATH can be ignored when pH of washing water is 8−10. And then total soda in fine ATH comprises lattice soda and soda in DSP, where soda in DSP can be calculated in terms of SiO_2 content in $Al(OH)_3$ based on the formula of DSP ($Na_2O{\cdot}Al_2O_3{\cdot}1.68SiO_2{\cdot}2H_2O$). Results of total soda content and soda content in DSP are given in Table 5.

Table 5 Variation of soda content in mass fraction in seeds and alumina trihydrate

Time/h	Sample 1		Sample 2	
	$w(Na_2O_T)$/%	$w(Na_2O_{DSP})$/%	$w(Na_2O_T)$/%	$w(Na_2O_{DSP})$/%
0	0.276	0.002	0.263	0.002
3	0.457	0.001	0.340	0.002
16	0.419	0.000	0.315	0.002
27	0.423	0.002	0.290	0.002
40	0.430	0.002	0.285	0.002
48	0.441	0.002	0.289	0.002

Na_2O_T: total soda content; Na_2O_{DSP}: soda content in DSP

Soda content in DSP is very low (≤0.002%) and stays constant in Table 5. The reason is that the solubility of DSP increases with the free alkali soda in solution, and that little SiO_2 exists in solution for great μ_{Si} (400±30) in pregnant liquor after desilication.

Without regard to the adsorption soda, lattice soda (Na_2O_{latt}) is equal to Na_2O_T subtracting Na_2O_{DSP} ($Na_2O_{latt}=Na_2O_T-Na_2O_{DSP}$). The dependence of the lattice soda content on time is plotted in Fig. 3.

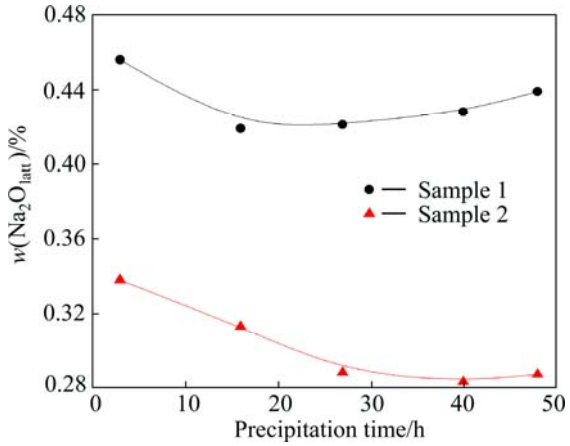

Fig. 3 Dependence of soda content in crystal on precipitation time

Results in Fig. 3 and Table 5 indicate that the total soda or lattice soda content in ATH is high in the initial period and decreases slowly with time. And this variation is in agreement with the variation of $d\eta/dt$ in Table 3 and PSD in Table 4, suggesting that $d\eta/dt$ and agglomeration affect remarkably the lattice soda. In addition, high temperature favors the reduction of the lattice soda content.

3.4 Influence of seed type on soda content

Species of seed also has remarkable effects on the precipitation of coarse ATH. Two species of seed are added for preparation of fine ATH. To prevent particle from agglomeration, aged seeds are added into precipitation tank, and the dependence of seeds on precipitation ratio can be seen in Fig. 4.

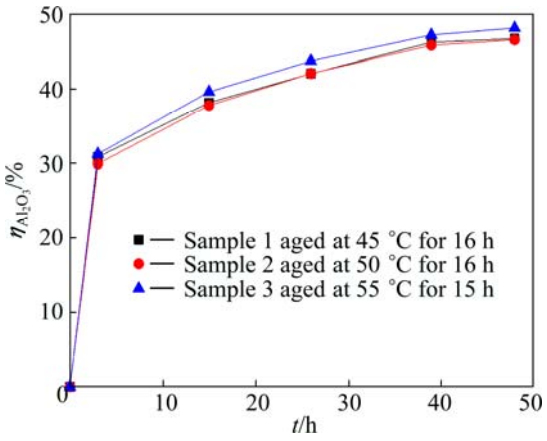

Fig. 4 Effect of seed type on precipitation ratio (Pregnant liquor: ρ_{Na_2Ok}=174.10 g/L; $\rho_{Al_2O_3}$=180.62 g/L; φ≈0.1; Variable temperature scheme: initial 55 °C, 45 °C after 15 h)

Figure 4 presents the dependence of the precipitation ratio on time. The regulation appears similar when different seeds are added. Precipitation ratio at initial period increases remarkably with the time due to the high super-saturation at low α_k (molar ratio of Na_2O to Al_2O_3), precipitation ratio at later period rises slowly with time, and precipitation ratio with different seeds at 48 h reach by ~48%.

Curves of precipitation ratio vs time in Fig. 4 are simulated, and these functions are then differentiated to obtain the precipitation rate (Table 6).

Table 6 Dependence of precipitation rate and time with different seeds added

Sample No.	Formula of simulation equation	$d\eta/dt$				
		3 h	15 h	26 h	39 h	48 h
1	$\eta_{Al_2O_3}=5.87\ln(1+56.05t)$	1.95	0.39	0.23	0.15	0.12
2	$\eta_{Al_2O_3}=6.14\ln(1+39.09t)$	2.03	0.41	0.24	0.16	0.13
3	$\eta_{Al_2O_3}=6.20\ln(1+46.97t)$	2.05	0.41	0.24	0.16	0.13

The precipitation rates (in Table 6) go down sharply at initial period. For example, the precipitation rates of sample 3 at 3 h, 15 h are 2.05, 0.41, respectively. And precipitation rate decreases slowly in the later period. Variation of the precipitation rate is similar to that in Table 3.

The PSD and the specific surface area at 3 h and 48 h are given in Table 7.

Table 7 shows that particle size increases slightly when precipitation undergoes from 3 h to 48 h, suggesting that aged seeds prevent particle from agglomeration at high temperature.

Effects of seed species on the total soda and soda in DSP are listed in Table 8.

Soda content in DSP varies from 0.001% to 0.007%. Results in Table 8 show that total soda content in the fine ATH is high at initial seeded precipitation and reduces slowly with time, and that total soda content in sample 3 is the least among samples 1, 2 and 3.

Table 7 Effect of seeds type on PSD and specific surface area

Sample No.	Time/h	PSD/μm			Specific surface area/($m^2 \cdot g^{-1}$)
		d(0.1)	d(0.5)	d(0.9)	
1	3	0.727	4.094	7.318	2.8
	48	0.774	4.289	7.674	2.643
2	3	0.758	4.498	7.980	2.61
	48	0.777	4.746	8.394	2.525
3	3	0.732	4.360	7.791	2.715
	48	0.736	4.482	8.042	2.685

Table 8 Effect of seeds type on soda content of seeds and alumina trihydrate

Time/h	Sample 1		Sample 2		Sample 3	
	$w(Na_2O_T)$/%	$w(Na_2O_{DSP})$/%	$w(Na_2O_T)$/%	$w(Na_2O_{DSP})$/%	$w(Na_2O_T)$/%	$w(Na_2O_{DS})$/%$_P$
0	0.280	0.005	0.250	0.001	0.245	0.002
3	0.350	0.002	0.356	0.004	0.337	0.003
15	0.290	0.004	0.296	0.003	0.296	0.001
26	0.275	0.002	0.286	0.007	0.276	0.001
39	0.288	0.000	0.265	0.002	0.275	0.005
48	0.293	0.002	0.269	0.005	0.275	0.001

The relationship between lattice soda and time is plotted in Fig. 5.

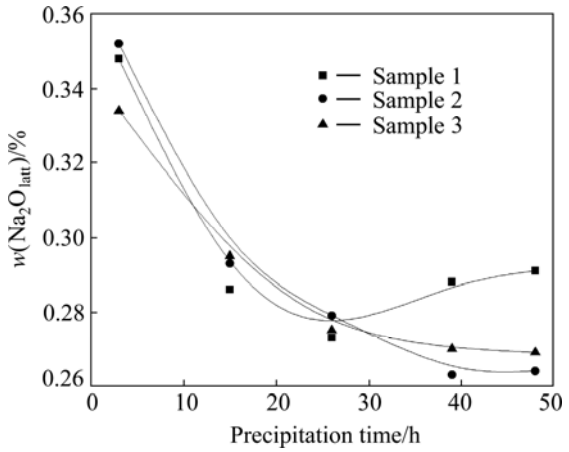

Fig. 5 Dependence of lattice soda content on precipitation time with different seeds added

The lattice soda contents of samples 1, 2 and 3 in Fig. 5 reduce significantly within 15 h, and then decrease slowly after 20 h. The results suggest that lattice soda relates to the precipitation rate for dη/dt declining sharply within 15 h in the seeded precipitation process (Table 6). It also implies that structure of aluminate solution affects the lattice soda content owing to 1) no remarkable agglomeration occurring; 2) concentration of alumina decreasing significantly.

3.5 Dependence of electrical conductivity on concentration of sodium aluminate

The concentration of Al_2O_3 decreases remarkably in the seeded precipitation process, and the aluminate anions present different structures at different concentrations. The structure of aluminate anions may influence the soda content of ATH in seeded precipitation process. The electrical conductivity of aluminate solution with a constant alkaline soda concentration ($\rho_{Na_2O_k}$= 160.14 g/L or 176.15 g/L) is then measured (Fig. 6).

As can be seen in Fig. 6, when $\rho_{Na_2O_k}$ is 160.14 g/L or 176.15 g/L, the electrical conductivity increases significantly with the rise of α_k , corresponding to the increase of α_k in the seeded precipitation process. The variation of electrical conductivity can be accounted for the decreasing aluminate anion though Na^+ concentration holds constant in seeded precipitation. Aluminate anions mainly exist in the forms of $Al(OH)_4^-$, some $Al_2O(OH)_6^{2-}$ and a little poly-aluminate ions in the solution with low α_k[13,14], in which Na^+, OH^- and $Al(OH)_4^-$ mainly account for the electrical conductivity [15]. And it suggests that the formation of ion pair $Na^+Al(OH)_4^-$ leads to the low electrical conductivity in the initial period of seeded precipitation at low α_k and high concentration of Al_2O_3, and that occurrence of less

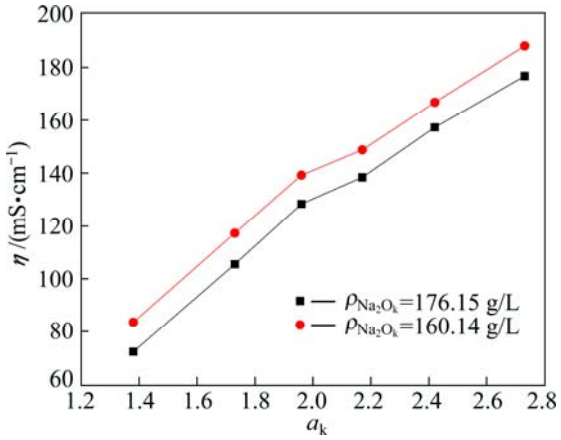

Fig. 6 Effect of caustic ratio (a_k) on electric conductivity of sodium aluminate solution at 25 °C

ion pair accounts for the high electrical conductivity in the late period of seeded precipitation with increasing α_k and constant Na^+. On the other hand, negative charge on the surface of ATH particles, resulting from the existence of oxygen atoms of hydroxyl group on the surface, adsorbs easily Na^+ of $Na^+Al(OH)_4^-$, so the remarkable variation of dη/dt can be observed in initial seeded precipitation process; it also implies that more Na^+ ions may remain in ATH in initial precipitation, resulting in high soda content of ATH. Correspondingly, less $Na^+Al(OH)_4^-$ and more free Na^+ in solution increase the electricity conductivity in the late period of seeded precipitation process, resulting in less adsorption of $Al(OH)_4^-$ on the surface of seeds, reducing dη/dt and soda content in ATH as well. But it needs further researches on the mechanism of Na^+ escaping from crystal and getting back into solution.

4 Conclusions

1) High concentration of aluminate solution, grinding circulative seeds, low temperature or high specific surface increases soda content in the fine ATH by seeded precipitation.

2) Soda mainly exists in form of lattice soda and less in DSP when the fine ATH is precipitated from sodium aluminate solution with $\rho_{Al_2O_3}$>160 g/L and μ_{Si}≈400. Particle agglomeration is limited with little seeds added. Lattice soda in the fine ATH reduces with increasing temperature, aged seeds and high precipitation rate.

3) High soda content in the fine ATH in the initial period and low soda content in late period of seeded precipitation may be related to variation of precipitation rate, precipitation ratio and formation of ion pair $Na^+Al(OH)_4^-$.

References

[1] YANG Zhong-yu. Alumina production technology [M]. Beijing: Metallurgical Industry Press, 1993: 126−132. (in Chinese)

[2] BHATTACHARYA I N, PARADHAN J K, GOCHHAYAT P K, DAS S C. Factors controlling precipitation of finer size alumina trihydrate [J]. International Journal of Mineral Processing, 2002, 65(2): 109−124.

[3] PARADHAN J K, GOCHHAYAT P K, BHATTACHARYA I N DAS S C. Study on the various factors affecting the quality of precipitated non-metallurgical alumina trihydrate particles [J]. Hydrometallurgy, 2001, 60(2): 143−153.

[4] FLEMING S D, ROHL A L, PARKER S C, PARKINSON G M. Atomistic modeling of gibbsite: Cation incorporation [J]. The Journal of Physical Chemistry B, 2001, 105(22): 5099−5105.

[5] FREIJ S J, PARKINSON G M. Surface morphology and crystal growth mechanism of gibbsite in industrial Bayer liquors [J]. Hydrometallurgy, 2005, 78(3): 246−255.

[6] LOH J S C, WATLING H R, PARKINSON G M. Alkali cations-role and effect in gibbsite crystallization [J]. Light Metals, 2002: 127−133.

[7] PRESTIDGE C A, AMEOV I. Cation effects during aggregation and agglomeration of gibbsite particles under synthetic Bayer crystallisation conditions [J]. Journal of Crystal Growth, 2000, 209(4): 924−933.

[8] BLAGOJEVIĆ I, BLEČIĆ D, VASILJEVIĆ R. Influence of decomposition parameters on agglomeration process and total soda content in precipitated Al $(OH)_3$ [J]. Journal of Crystal Growth, 1999, 200(3): 558−564.

[9] GAN Y, FRANKS G V. Charging behavior of the gibbsite basal (001) surface in NaCl solution investigated by AFM colloidal probe technique [J]. Langmuir, 2006, 22(14): 6087−6092.

[10] HALEEN L W, PEEASON A. Precipitation of aluminum oxide having low sodium oxide content: US4014985 [P]. 1977−03−29.

[11] BROWN G P, WOOD D G. Production of low soda alumina: US5529761 [P]. 1996−06−25.

[12] LI Jun, CLIVE A, JONAS P, ADDAI-MENSAH J. Secondary nucleation of gibbsite crystals from synthetic Bayer liquors: Effect of alkali metal ions [J]. Journal of Crystal Growth, 2000, 219(4): 451−464.

[13] SIPOS P. The structure of Al (III) in strongly alkaline aluminate solutions—A review [J]. Journal of Molecular Liquid, 2009, 146: 1−14,

[14] MOOLENAAR R J, EVANS J C, MCKEEVER L D. Structure of the aluminate ion in solutions at high pH [J]. Journal of Physical Chemistry, 1970, 74(20): 3629−3636.

[15] LI Xiao-bin, WANG Dan-qin, LIANG Shuang, LIU Gui-hua, PENG Zhi-Hong, ZHOU Qiu-Sheng. Relationship between electric conductivity and ion structure of sodium aluminate solution [J]. Chemical Journal of Chinese Universities, 2011, 21(10): 1651−1655.

种分制备超细氢氧化铝中碱含量的变化

刘桂华，王 鹏，齐天贵，李小斌，田 侣，周秋生，彭志宏

中南大学 冶金与环境学院，长沙 410083

摘 要：种分氢氧化铝中碱含量变化规律关系到氢氧化铝的质量和碱耗，通过测定溶液浓度和电导率、氢氧化铝中碱含量和粒度分布以及分析粒子形貌，研究种分氢氧化铝中碱含量的变化规律。结果表明，溶液组分浓度高、球磨晶种循环、种分温度低、初始分解速率快或产品比表面积大都会导致氢氧化铝中碱含量升高；在低硅铝酸钠溶液种分过程中，粒子的附聚得到抑制，超细氢氧化铝中碱主要以晶格碱形式存在，以钠硅渣形式存在的碱含量极低；同时，升高初始分解温度，晶种老化，降低分解速率，延长种分时间，都有利于产品中碱含量的降低。结果还表明：种分过程中，$Na^+Al(OH)_4^-$离子可能对产品中碱含量有很大的影响。

关键词：氢氧化铝；种分；碱含量；晶格碱；铝硅酸钠溶液

(Edited by Hua YANG)